CHD4/Mi-2β activity is required for the positioning of the mesoderm/ neuroectoderm boundary in *Xenopus*

Britta Linder,[1] Edith Mentele,[1] Katrin Mansperger,[1] Tobias Straub,[1] Elisabeth Kremmer,[2] and Ralph A.W. Rupp[1,3]

[1]Adolf-Butenandt-Institut, Institut für Molekularbiologie, Ludwig-Maximilians-Universität, 80336 München, Germany; [2]GSF-Forschungszentrum, Institut für Molekulare Immunologie, 81377 München, Germany

Experiments in *Xenopus* have illustrated the importance of extracellular morphogens for embryonic gene regulation in vertebrates. Much less is known about how induction leads to the correct positioning of boundaries; for example, between germ layers. Here we report that the neuroectoderm/mesoderm boundary is controlled by the chromatin remodeling ATPase CHD4/Mi-2β. Gain and loss of CHD4 function experiments shifted this boundary along the animal–vegetal axis at gastrulation, leading to excess mesoderm formation at the expense of neuroectoderm, or vice versa. This phenotype results from specific alterations in gene transcription, notably of the neural-promoting gene *Sip1* and the mesodermal regulatory gene *Xbra*. We show that CHD4 suppresses *Sip1* transcription by direct binding to the 5′ end of the *Sip1* gene body. Furthermore, we demonstrate that CHD4 and Sip1 expression levels determine the "ON" threshold for Nodal-dependent but not for eFGF-dependent induction of *Xbra* transcription. The CHD4/Sip1 epistasis thus constitutes a regulatory module, which balances mesoderm and neuroectoderm formation.

Xenopus as an embryological model organism has contributed extensively to our understanding of vertebrate development, in particular with regard to the impact of growth factor gradients on embryonic patterning (see Green 2002). A small set of signaling cascades—driven by Wnt, BMP, Nodal, and FGF ligands—has emerged as the early signals, which act in a temporally and spatially coordinated manner to establish the basic vertebrate body plan (Heasman 2006; Kimelman 2006). In recent years, these growth factors have been joined by a diverse group of extracellular inhibitors of Wnt, BMP, and Nodal proteins, which are secreted by the Spemann-Mangold organizer (De Robertis and Kuroda 2004; Niehrs 2004). These inhibitors shape and refine the growth factor gradients into dynamic, overlapping signaling territories, which have been visualized in situ by tracing activated, intracellular components of the different signaling pathways (Schohl and Fagotto 2002). In addition, the sophisticated use of the "animal cap" system for embryonic induction experiments (for review, see Green 1999) has been extraordinarily helpful to reveal epistatic relationships between signals and target genes. Together, these approaches have established a regulatory blueprint of the cellular differentiation programs within the developing frog embryo (Loose and Patient 2004).

Naturally, this molecular and genetic description of the early development of *Xenopus* is far from being complete. With respect to embryonic patterning, we still have a rather limited understanding of how signals become transformed into sharply demarcated gene expression domains. Current knowledge indicates that many, if not most, "immediate early" genes receive a complex regulatory input. A paradigm for combinatorial regulation is provided by the *Xenopus brachyury* (*Xbra*) gene, which is required for mesoderm formation in vertebrates. *Xbra* transcription is locally induced in the prospective mesoderm of the embryo shortly before gastrulation in response to Nodal/Smad2 and FGF/MAPK (mitogen-activated protein kinase) signaling (for review, see Wardle and Smith 2006). Detailed analysis of the *Xbra* regulatory contig has indicated that its typical ring-like expression domain is generated by a rather general transcriptional activation combined with active transcriptional repression in regions that do not require Xbra protein function (Latinkic et al. 1997; Lerchner et al. 2000). A similar conclusion has recently been derived from experiments with frog embryos, in which protein synthesis

had been blocked by cycloheximide. Under these conditions, abnormal spreading of mesodermal gene expression domains was observed, which was interpreted to reflect the absence of de novo synthesized repressors (Kurth et al. 2005). Together, these studies illustrate the fundamental importance of repression for the regional induction of gene expression.

Potential repressors of *Xbra* transcription include the proteins Goosecoid, Otx2, and Mix1, which bind to homeodomain-binding sites near the *Xbra* promoter (Latinkic et al. 1997). This region contains also a single bipartite binding site for the Smad-interacting protein Sip1 (Verschueren et al. 1999; Eisaki et al. 2000; Lerchner et al. 2000; Papin et al. 2002). Sip1 belongs to the δEF1 family of proteins, which are involved in cell fate decisions in *Drosophila* and vertebrates (Postigo and Dean 1997). Mutations in the human *Sip1* gene cause a form of Hirschsprung's disease, associated with mental retardation, microcephaly, and facial abnormalities (Wakamatsu et al. 2001). Sip1 was originally identified through its ability to interact with receptor-regulated Smad proteins. Gel-shift analyses showed that Sip1 binds to 5′-CACCT-3′ DNA sequences of various promoters, including that of *Xbra* (Verschueren et al. 1999; Papin et al. 2002). When overexpressed in *Xenopus* animal caps, Sip1 displays neural-inducing activity (Eisaki et al. 2000; Nitta et al. 2004). Consistent with this, work in chick embryos has placed Sip1 into a pathway operating during gastrulation, in which FGF indirectly induces the transcription factor Churchill, which induces Sip1, which, in turn, represses mesoderm formation and promotes neurogenesis (Sheng et al. 2003). In the frog, *Xbra* and *Sip1* are initially coexpressed at the onset of gastrulation, but quickly refine into adjacent expression domains representing mesoderm and neuroectoderm (Papin et al. 2002). The mechanism by which this separation occurs is not known, but most likely is pivotal for formation and positioning of the boundary between these two germ layers.

Ample evidence supports the notion that the transcriptional activity of genes is mechanistically coupled to their local chromatin structure. The chromatin environment is regulated by two classes of enzymes, which either catalyze covalent modifications of histone tails or hydrolyze ATP to mobilize nucleosomes. Vertebrates contain a set of ~30 nucleosome-stimulated ATPases related to the prototypic SNF2 protein from yeast (Linder et al. 2004). These ATPases represent the enzymatic core subunits of conserved multiprotein nucleosome remodeling machines (Becker and Hörz 2002). Recently, several groups have simultaneously described the protein composition of one of these machines, most often referred to as the NuRD complex (for review, see Bowen et al. 2004). This complex shows both remarkable conservation among metazoa as well as heterogeneity at the individual protein subunit level. In addition to its core ATPase CHD4/Mi-2β, which is required for nucleosome sliding/remodeling, the NuRD complex contains histone deacetylases (HDACs) and members of the MBD family of methyl-CpG-binding proteins. By this unique protein composition, NuRD may couple DNA methylation to chromatin remodeling and histone deacetylation (Wade et al. 1999). Detailed analyses in diverse model organisms and cell culture systems have emphasized the importance of NuRD as a versatile transcriptional repressor complex, which regulates cell type-specific transcriptional programs at the chromatin level (Kehle et al. 1998; von Zelewsky et al. 2000; Unhavaithaya et al. 2002; Fujita et al. 2003, 2004).

The dynamic mRNA expression patterns of the *Xenopus* orthologs of the mammalian SNF2-like ATPases during early embryogenesis (Linder et al. 2004) have suggested that quantitative and/or qualitative differences in nucleosome-remodeling activities between cells could be of regulatory importance for embryonic gene regulation. In this study, we have tested this assumption by performing gain- and loss-of-function experiments for the *Xenopus* CHD4-ATPase. Our results place CHD4/Mi-2β activity at the top of a regulatory cascade, which determines the position of the neuroectoderm/mesoderm border along the animal–vegetal axis of the gastrula embryo by controlling specifically the Activin/Nodal input for *brachyury* transcription.

Results

Interference with CHD4 protein activity affects specific mesodermal and neuroectodermal gene expression domains

Nonuniform expression of the *xCHD4* mRNA during frog embryogenesis (see Supplementary Fig. S1 and Linder et al. 2004) suggested that it could be selectively involved in regional gene regulation from early gastrula stages onward. To test this assumption, we used several independent approaches of functional interference with CHD4 protein activity. We created a dominant-negative variant of the CHD4-ATPase (dnCHD4) by point-mutating the lysine residue at position 748 to arginine. The analogous mutation in the SNF2 ATPase maintains the integrity of the yeast SWI/SNF chromatin remodeling complex, but abolishes transcriptional activation of target genes (Richmond and Peterson 1996). While injection of wild-type *CHD4* mRNA (*wtCHD4*) would be expected to increase CHD4/NuRD activity, overexpression of the *dnCHD4* variant should inhibit endogenous CHD4 protein functions by competition. For loss-of-function analysis, we designed a Morpholino oligonucleotide (Heasman et al. 2000), complementary to the translational start site of the *CHD4* mRNA (*CHD4*-Mo) (see Supplementary Fig. S2). This antisense oligonucleotide inhibited endogenous *CHD4* mRNA translation both in vitro and in vivo, while an unrelated control Morpholino oligonucleotide had no effect (Supplementary Fig. S2; data not shown).

After injecting the various reagents singly into one blastomere at the two-cell stage, we cultured control and injected embryo populations until gastrula stage, when they were fixed for RNA in situ hybridization. We analyzed a total of 14 genes, which mark specific areas within the developing embryo. These included *chordin*

(*chd*), nodal-related-3 (*xnr3*), *vent2*, *Sip1*, *Xbra*, *Wnt11*, *MyoD* (see Fig. 1), and *noggin*, *goosecoid* (*gsc*), *vent-1*, *mixer*, *dickkopf*, *otx-2*, and *mix1* (data not shown). Among those, the mesodermal markers *Xbra*, *MyoD*, and to a lesser extent also *Wnt11*, were down-regulated in the majority of the *CHD4*-Mo-injected embryos in several independent experiments (Fig. 1, right column; for phenotypic penetrance, see Supplementary Fig. S3). No perturbation of mesodermal gene expression patterns was observed upon injection of an unrelated control Morpholino (data not shown). In contrast, embryos in-
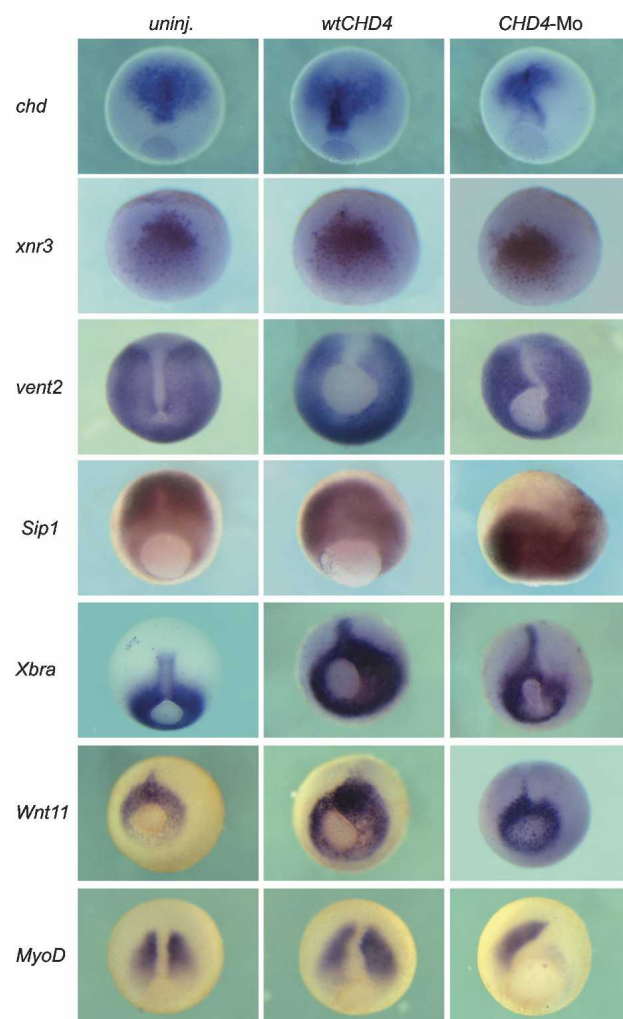

Figure 1. Perturbation of CHD4 activity leads to specific alterations in gastrula gene expression. Embryos were unilaterally injected with a dose of 1.0 ng of *CHD4* mRNA or 40 ng of *CHD4*-Mo into one blastomere at the two-cell stage. At gastrula stages, they were fixed, presorted into left-side- or right-side-injected populations by fluorescence of coinjected eGFP (not shown), and used for RNA in situ hybridizations for the marker genes indicated to the *left*. Displayed are representative embryos from three to five independent experimental repeats, in which the *left* side serves as an internal control for normal marker gene expression, while the *right* side shows the expression under the experimental condition (either vegetal or dorso-vegetal views). The injected side is to the *right*.

jected with *wtCHD4* mRNA (Fig. 1, middle column; Supplementary Fig. S3) showed a strong, unilateral expansion of *Xbra* transcripts toward the animal pole. A somewhat milder expansion was also observed for *Wnt11* and *MyoD*.

Injections of *dnCHD4* mRNA caused a comparable reduction of the *Xbra* expression domain on the injected side like the *CHD4*-Mo, and both phenotypes were rescued by coinjection of *wtCHD4* mRNA (see Fig. 2A; Supplementary Fig. S3). We also targeted the Morpholinos, *wtCHD4* and *dnCHD4* mRNAs specifically to the dorsal (dmz) or ventral marginal zone (vmz) by injection of single blastomeres at the four-cell stage, and stained the embryos for *Xbra* mRNA (data not shown). Vmz-injected embryos showed normal expression of *Xbra*, while in dmz-injected embryos we observed a slight reduction in the dorsal-most quadrant of the *Xbra* expression domain, but only at the highest dose of *CHD4*-Mo oligo tested (60 ng). Together, these observations indicate that CHD4 controls mainly the dorsolateral aspect of the *Xbra* expression domain.

The RNA in situ analysis also indicated misexpression of the neural plate marker *Sip1*. Most embryos injected with *wtCHD4* mRNA showed a significant, local reduction of *Sip1* transcripts in the prospective neural plate, whereas the *Sip1* expression domain was expanded both animally and laterally in *CHD4*-Mo-injected embryos (Fig. 1; Supplementary Fig. S3). Coinjection of *wtCHD4* mRNA and *CHD4*-Mo resulted in mostly normal *Sip1* expression, indicating that these phenotypes are specific and depend on CHD4 protein abundance (Fig. 2A; Supplementary Fig. S3). The altered *Xbra* and *Sip1* expression domains caused by *wtCHD4* overexpression could not be rescued upon the coinjection of a control Morpholino (Fig. 2A; data not shown). To obtain independent quantitative evidence that CHD4 regulates *Sip1* transcription, we overexpressed CHD4 protein in animal cap explants. As little as 0.25 ng of *wtCHD4* mRNA was sufficient to suppress *Sip1* mRNA levels to ~50% of uninjected control explants, while even 1.0 ng of *CHD4* mRNA was not sufficient to silence *Sip1* transcription completely (see Fig. 2B).

Most of the tested genes, however, were practically unaffected by these conditions, even though some domains (e.g., chd, vent2) (see Fig. 1) appear distorted near the dorsal midline. Since Xbra and its target gene Wnt11 control cell behavior in the dorsal mesoderm during involution (Kwan and Kirschner 2003), we interpret this distortion to reflect a perturbed midline formation due to *Xbra/Wnt11* misexpression, rather than a CHD4-dependent phenotype. Taken together, this analysis indicates a striking selectivity of target genes, which respond to perturbations of CHD4 activity. In summary, *Sip1* responded reciprocally to alterations of CHD4 activity, compared with the affected mesodermal genes. Most reports link CHD4/Mi-2β to chromatin-mediated transcriptional silencing (Bowen et al. 2004). Since on one hand Sip1 is known to repress the *Xbra* promoter (Papin et al. 2002), and on the other hand Xbra has been shown to be sufficient for mesoderm differentiation (Cunliffe
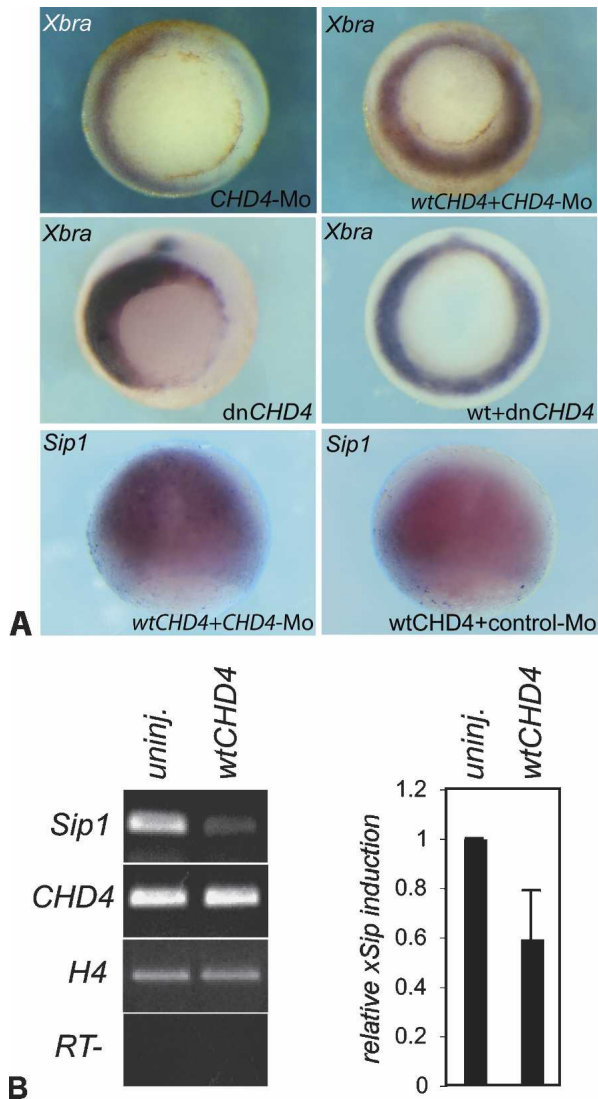
Figure 2. CHD4 regulates *Sip1* and *Xbra* mRNA expression specifically. CHD4 overexpression suppresses Sip1 mRNA levels in animal cap explants. (*A*) Rescue of *Xbra* and *Sip1* mRNA expression at mid-gastrula (injections and embryo presentation as in Fig. 1). *CHD4*-Mo (40 ng) or *dnCHD4* mRNA (1.0 ng) causes similar inhibition of *Xbra* mRNA on the injected side, which is rescued by coinjection of *wtCHD4* mRNA (1.0 ng). Unilateral reduction of Sip1 mRNA in the prospective neural plate area is rescued by CHD4-Mo, but not Control-Mo, coinjection. The injected side is to the *right*. (*B, left* panel) Semiquantitative RT–PCR; 1.0 ng of *wtCHD4* mRNA was injected. (*Right* panel) Real-time RT–PCR quantification of *Sip1* mRNA levels after normalization to histone *H4*; 0.25 ng of *wtCHD4* mRNA was injected.

and Smith 1992), the embryonic phenotypes suggested an epistasis between *CHD4*, *Sip1*, and *Xbra*, which we decided to investigate further.

CHD4 expression levels define the boundary between neuroectoderm and mesoderm

In normal development, the *Sip1* and *Xbra* expression domains overlap initially in the dorsal marginal zone,

but then become quickly separated. At the end of gastrulation, *Sip1* is expressed strongly in the neuroectoderm and to a lesser extent in the mesoderm, while *Xbra* mRNA is restricted to prospective mesoderm (Papin et al. 2002). This raised the issue of whether CHD4 takes part in the process that separates the *Sip1* and *Xbra* domains, or whether CHD4 controls a separate aspect of their regulation.

To address this question, we sectioned gastrula embryos and stained them separately for *Xbra* or *Sip1* mRNA (see Fig. 3A). Attempts to stain embryos simultaneously for both transcripts have failed repeatedly, probably due to the different *Sip1* and *Xbra* mRNA abundances. We found that the *Xbra* domain was enlarged at the expense of the *Sip1* domain in embryos overexpressing CHD4 protein, and vice versa in embryos injected with *CHD4*-Mo. Injecting *wtCHD4* mRNA and *CHD4*-Mo together resulted mostly in embryos with normal proportions of *Xbra* and *Sip1* expression (Supplementary Fig. S3). However, neither *Sip1* nor *Xbra* mRNAs spread into the underlying endoderm (Fig. 3A). This indicates that CHD4 specifically controls the position of the mesoderm/neuroectoderm boundary along the animal–vegetal axis.

To determine which impact the early imbalance between *Xbra* and *Sip1* expression might have on later development, we examined both the histology and the expression of differentiation markers in sections from unilaterally injected tadpoles (see Fig. 3B,C; Supplementary Fig. S3). Due to the relative morphogenetic movements of mesoderm and neuroectoderm along the rostrocaudal axis, the observed phenotypes were most pronounced in the eye and the trunk somites, respectively. *WtCHD4*-overexpressing embryos were characterized by reduced or absent eyes (Fig. 3B, top left), accompanied by significantly enlarged myotomes (Fig. 3B, top right). Both phenotypes were rescued by coinjection of *dnCHD4* mRNA (Supplementary Fig. S3; data not shown). In contrast, *CHD4*-Mo-injected embryos displayed a hyperproliferative retina; the somites of these embryos, however, contained loosely packed cells and were locally disorganized and smaller than ipsilateral, uninjected somites (cf. Fig. 3B, bottom panels). All of these embryos contained normal-looking notochords, consistent with the observation that gene expression in the gastrula organizer was unaffected by CHD4 (see above). Furthermore, expression of neural (*nrp1*) and mesodermal (*muscle-actin*) differentiation markers was confined to the proper domains, indicating that the affected tissues contained correctly specified cells (Fig. 3C). In toto, these results suggest that the early alterations of gene expression patterns by the specific perturbation of CHD4 cannot be compensated during development, but have lasting consequences for the embryo.

CHD4 binds to the Sip1 gene

The combined results of Figures 2B and 3A suggest that suppression of *Sip1* transcription by CHD4 determines the animal border of the domain, in which *Xbra* can be
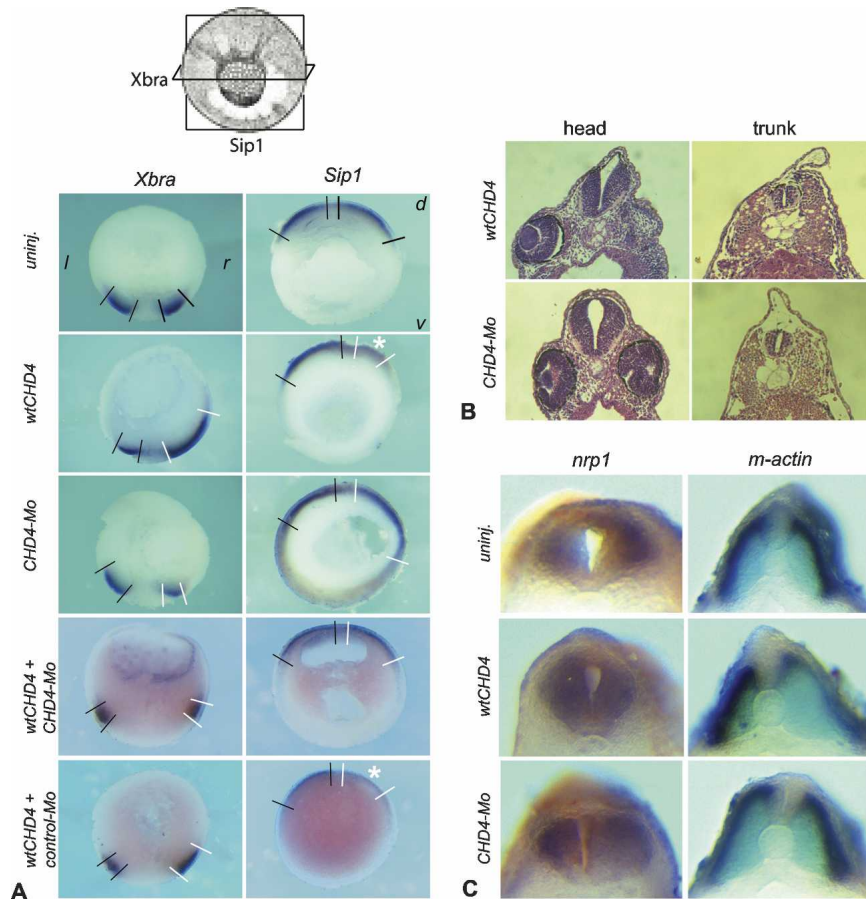
Figure 3. *CHD4* levels define the position of the mesoderm/neuroectoderm boundary. Embryos were unilaterally injected with the reagents indicated on the *left*. In each panel, the *right* side was injected, and the *left* side serves as internal control. In *A* and *C*, embryos were subjected to in situ hybridization for the indicated markers prior to sectioning. (*A*) Gastrula embryos, stained for endogenous *Xbra* and *Sip1* mRNAs, were bisected as indicated in the cartoon. Black bars delimit the normal expression domains, and white bars mark the domains in the injected halves. (d) Dorsal; (v) ventral; (l) left; (r) right. Note reduced *Sip1* staining in *wtCHD4*-injected embryos (white asterisks). (*B*) Transverse, hematoxylin-and-eosin-stained sections of tailbud-stage embryos at the head (*left* column) or anterior trunk (*right* column) level. *WtCHD4*-injected embryos showed absent or reduced eyes but enlarged somites on the injected side. *CHD4*-Mo-injected embryos showed hyperproliferation of the retina and disorganized, loosely packed somites on the injected side. (*C*) Hindbrain and trunk somites of either wt*CHD4* mRNA or *CHD4*-Mo-injected embryos express cognate differentiation markers in neural (nrp1) and muscle (m-actin) tissues.

induced. To obtain evidence for a direct regulation of *sip1* by CHD4, we performed chromatin immunoprecipitation (ChIP) experiments. The structural organization of the mouse *sip1* locus has been described recently (Nelles et al. 2003), including the presence of nine untranslated and alternatively spliced exons (U1–U9), and the nucleotide sequence of two putative promoter regions located upstream of U1 and U4/U5, respectively. Among these elements, cDNA and genomic *sip1* DNA sequences from *Xenopus* (see Materials and Methods for details) showed high sequence similarity for exons U5, E1, and E2, while shorter stretches of clearly conserved DNA sequence extended into the promoter region upstream of U5 (see Fig. 4A). Based on this information, we derived several primer pairs for quantitative PCR analysis of the *Xenopus sip1* gene.

The amplicons xU5, xE1, and xE2 cover ~90 kb of the transcribed 5′ portion of the *xsip1* gene. Using chromatin fragments from mid-gastrula *Xenopus* embryos, we precipitated endogenous CHD4 protein and normalized its relative occupancy at these sites to a control amplicon located within the active *GAPDH* gene. A second control amplicon lies within the promoter region of the *xTH/bZIP* gene, which is not transcribed during frog embryogenesis until metamorphosis (Furlow and Brown 1999). In three out of three experiments, we found that CHD4 binding was more than threefold enriched at the

xE1 amplicon; that is, within the 5′ part of the transcribed gene body (Fig. 4B). These results identify the *sip1* gene as a direct target of CHD4 in the embryo at the developmental stage when the boundary between mesoderm and neuroectoderm is formed.

CHD4 controls the dose response of the Xbra promoter to Activin

Our results describe a regulatory pathway in which CHD4 directly suppresses *Sip1* transcription to a level that prevents activation of *Xbra* in the prospective neural plate, but is permissive for its induction in the prospective mesoderm. The *Xbra* promoter has been shown to be inducible by eFGF and low concentrations of Activin, and to be maintained through an indirect feedback loop, in which Xbra protein induces *eFGF* expression, which in turn again stimulates *Xbra* transcription (Latinkic et al. 1997; Casey et al. 1998). The same Activin/FGF-sensitive promoter region contains also a binding site through which Sip1 represses *Xbra* in the dorsal animal hemisphere (Papin et al. 2002). This detailed insight into *brachyury* regulation provided us with the opportunity to investigate the interplay of CHD4 and Sip1 activities with growth factor signals.

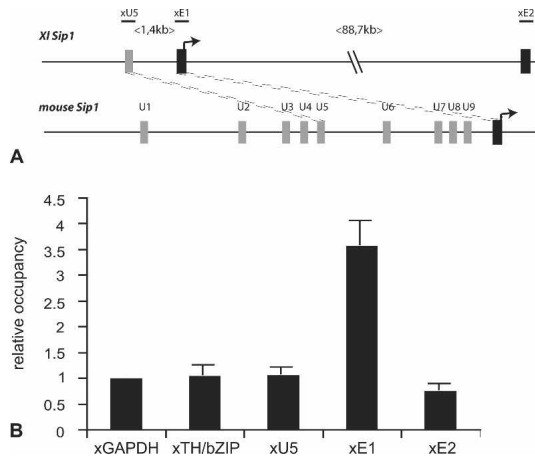In a first experimental series, we injected increasing amounts of *Activin* mRNA into the animal hemisphere

Figure 4. CHD4 binds to the *Sip1* gene. (*A*) The cartoon depicts the organization of frog and mouse *Sip1* gene loci around the first translated exon E1 (AUG indicated by arrow). While exons U5 and E1 are highly conserved in sequence (connected by dashed lines), mouse exons U6–U9 apparently are not conserved in *Xenopus*. Black bars indicate the relative positions of the ChIP amplicons xU5, xE1, and xE2 for *Xenopus*. Not drawn to scale; however, absolute distances between ChIP probes are given in brackets. (*B*) ChIPs were performed on mid-gastrula *Xenopus* embryos (NF11), using a rat monoclonal antibody mix against xCHD4 protein followed by real-time PCR analysis. They revealed preferential binding of endogenous xCHD4 protein to E1 (*n* = 3 independent experiments). The relative xCHD4 occupancy was normalized to the xGAPDH amplicon; xTH/bZIP is a silent gene, which becomes activated during metamorphosis. Error bars are the mean standard deviation.

of the four-cell-stage embryo, dissected animal caps, and assessed the resulting *Xbra* mRNA levels by semiquantitative RT–PCR at the early gastrula stage. A minimal dose of 16 pg of *Activin* mRNA was necessary to reproducibly induce *brachyury* transcription over basal levels (Fig. 5A,B, lanes 1–4 each). This threshold response became significantly altered when we simultaneously manipulated CHD4 activity in the explants. Upon coinjection of *wtCHD4* mRNA, *Xbra* was activated already by 1pg of *Activin* mRNA (Fig. 5A, lanes 5–8). In contrast, when *CHD4*-Mo was coinjected, even 24 pg of Activin failed to induce the *Xbra* promoter (Fig. 5B, cf. lanes 4 and 8).

These effects were both selective and specific for several reasons. First, Activin-dependent induction of other genes like *gsc* was unaltered by CHD4 overexpression (Fig. 6B), as was induction of *siamois* and *xnr3* transcription by canonical Wnt signaling (Fig. 6D). Second, the Activin/Smad signaling pathway remained functional in the presence of *CHD4*-Mo, since *Xbra* could still be induced by higher Activin amounts (100 pg) (Fig. 5B, lane 9). Third, the inhibition of *Xbra* induction by *CHD4*-Mo was overcome by coinjection of *wtCHD4* mRNA in a dose-dependent manner (Fig. 6A). Most notably, however, the normal Activin dose response of the *Xbra* promoter was restored by compensatorial manipulations of Sip1 protein abundance. Specifically, the sensitization of the *Xbra* promoter caused by CHD4 overexpression was

reverted by coinjecting *Sip1* mRNA (Fig. 5A, lanes 9–13), while its *CHD4*-Mo-dependent desensitization was rescued by inhibiting endogenous Sip1 protein translation (Fig. 5B, lanes 10–14) with a Sip1-specific Morpholino oligonucleotide (Nitta et al. 2004). Additionally, the desensitizing effect of *CHD4*-Mo injection on *Xbra* expression could be converted upon the coinjection of *CHD4* mRNA (Fig. 6A).

The key observations of these experiments were confirmed by real-time RT–PCR analysis in two additional, independent experiments. Specifically, this included the sensitized induction response of the *Xbra* promoter and its rescue by *Sip1* mRNA (Fig. 5C). We also show here that *dnCHD4* mRNA efficiently antagonizes the sensitized promoter response induced by wtCHD4 protein. Furthermore, the Xbra induction response to a higher Activin dose was again significantly suppressed by both *dnCHD4* mRNA and *CHD4*-Mo, and the latter effect was at least partly reversed by *Sip1*-Mo (Fig. 5D).

Finally, we injected increasing amounts of *eFGF* mRNA, either alone or in combination with *CHD4* mRNA or *CHD4*-Mo (Fig. 6C). In this case, alterations in CHD4 abundance had no significant effect on the eFGF/MAPK-dependent stimulation of the *Xbra* promoter. Together, these results indicate that CHD4 selectively controls, in a Sip1-dependent manner, the "ON" threshold of the *Xbra* promoter for Activin/Nodal-like induction; that is, the primary signal that initiates *brachyury* transcription and mesoderm formation (for review, see Kimelman 2006).

Discussion

This study describes a surprising role for the CHD4/Mi-2β ATPase during germ layer formation; that is, it balances the relative proportions of mesodermal and neuroectodermal territories, which arise through morphogen-mediated inductions (De Robertis and Kuroda 2004; Stern 2005; Heasman 2006). CHD4 achieves this function by influencing the regulatory interplay of the *Xbra* and *Sip1* genes at the early gastrula stage, which refines the expression domains of these key regulators of mesodermal and neuronal cell fates (Papin et al. 2002; Sheng et al. 2003; Nitta et al. 2004). Remarkably, CHD4-dependent interference with the Sip1/Xbra module leads to stable, disproportionate differentiation of mesodermal and neural tissues.

With regard to the underlying mechanism, we have shown that CHD4 suppresses *Sip1* transcription both in the embryo and in animal cap explants, through direct interaction targeted at the *Sip1* 5′ gene body. Interestingly, the presence of CHD4 in the vicinity of the *Sip1* promoter modulates the expression of this gene rather than imposing a full transcriptional "OFF" state. This regulatory mode is reminiscent of the paradigm described for the *xHairy2A* gene, where the methyl-CpG-binding protein MeCP2 together with the SMRT corepressor complex modulates transcription in a dynamic manner without complete silencing (Stancheva et al. 2003). Such regulation may be prominently used in un-
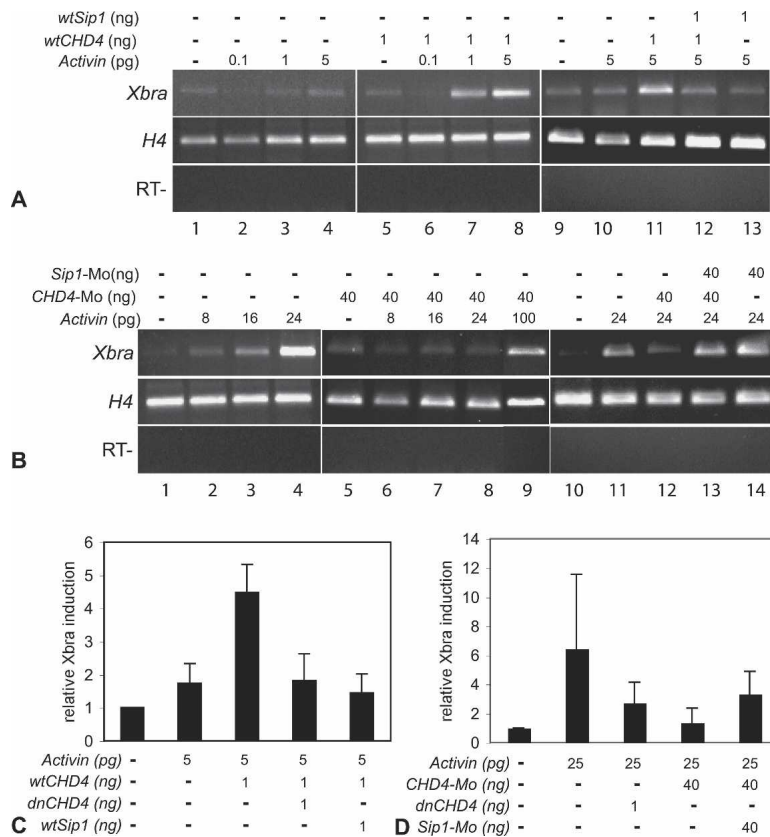
A

wtSip1 (ng)	-	-	-	-	-	-	-	-	-	-	-	1	1
wtCHD4 (ng)	-	-	-	-	1	1	1	1	-	-	1	1	-
Activin (pg)	-	0.1	1	5	-	0.1	1	5	-	5	5	5	5

Xbra
H4
RT-

1 2 3 4 5 6 7 8 9 10 11 12 13

B

Sip1-Mo(ng)	-	-	-	-	-	-	-	-	-	-	-	-	40	40
CHD4-Mo (ng)	-	-	-	-	40	40	40	40	40	-	-	40	40	-
Activin (pg)	-	8	16	24	-	8	16	24	100	-	24	24	24	24

Xbra
H4
RT-

1 2 3 4 5 6 7 8 9 10 11 12 13 14

C

relative Xbra induction

Activin (pg)	-	5	5	5	5
wtCHD4 (ng)	-	-	1	1	1
dnCHD4 (ng)	-	-	-	1	-
wtSip1 (ng)	-	-	-	-	1

D

relative Xbra induction

Activin (pg)	-	25	25	25	25
CHD4-Mo (ng)	-	-	-	40	40
dnCHD4 (ng)	-	-	1	-	-
Sip1-Mo (ng)	-	-	-	-	40

Figure 5. CHD4 defines the activation threshold for Activin-dependent *Xbra* induction. Animals cap explants, preloaded with various mRNAs and Morpholinos as indicated, were lysed at mid-gastrula and analyzed for *Xbra* mRNA by RT–PCR. Histone H4 served as loading control; RT– represents mock RT–PCR reactions without reverse transcriptase. (*A*) Overexpression of CHD4 protein sensitized the *Xbra* promoter for Activin induction in a Sip1-dependent manner. Note that *Xbra* was hardly induced by 5 pg of *Activin* mRNA alone (lane *4*), but already by 1 pg of Activin mRNA, when *CHD4* mRNA was coinjected (lane *7*). The CHD4-dependent sensitization of the *Xbra* gene was reverted by coinjection of *Sip1* mRNA. (*B*) Partial ablation of CHD4 protein by Morpholino knockdown desensitized *Xbra* for Activin induction. Note that *CHD4*-Mo-injected caps still expressed only basal *Xbra* mRNA levels at an inducer dose of 24 ng of Activin mRNA (cf. lanes *4* and *8*), while at 100 pg induction was partially restored (lane *9*). The observed desensitization was reverted by coinjection of *Sip1*-Mo (cf. lanes *12* and *13*). These key observations were confirmed in two additional, independent experiments by real-time RT–PCR quantification: (*C*) The wtCHD4-dependent sensitization of the *Xbra* promoter response is inhibited by either *dnCHD4* or *Sip1* mRNA coinjection. (*D*) Both *dnCHD4* and *CHD4*-Mo desensitize the *Xbra* promoter; *Sip1*-Mo coinjection partially rescues the *CHD4*-Mo down-regulation of Xbra induction. *Xbra* mRNA levels were normalized to histone H4 and uninjected control explants.

committed, pluripotent cells, which have to sort out small differences of morphogen signals.

The resulting *Sip1* expression levels, in turn, specifically control the sensitivity of the *Xbra* promoter for Activin/Nodal-like signals. Our data do not exclude additional functions of CHD4 during development, but identify the CHD4/Sip1 epistasis as a pivotal regulatory module in the formation of the boundary between mesoderm and neuroectoderm. It will be interesting to determine whether *CHD4* transcription itself is induced or repressed by growth factor signals, which is suggested by its nonuniform transcription in the embryo (Supplementary Fig. S1; Linder et al. 2004).

The above statements on CHD4 function rest on several lines of independent evidence. First, we observed that an increase in wild-type CHD4 protein levels caused phenotypes that were opposite to those achieved either by reducing endogenous CHD4 protein levels through a CHD4-specific antisense Morpholino strategy, or by overexpressing an ATPase-minus CHD4 protein variant. Secondly, the phenotypes of the *CHD4*-Mo-injected embryos were rescued by coexpression of wild-type CHD4 protein both on the morphological and molecular levels (Figs. 2, 3, 5, 6; Supplementary Fig. S3). In addition, the majority of tested genes (12 of 16) were expressed fairly normally under the various experimental conditions, strongly arguing against an unspecific perturbation of cellular transcription or of bulk chromatin architecture. Since most of these genes are regulated by Wnt, FGF,

BMP, or Nodal signals, we conclude that the major embryonic signaling pathways remained fully functional, and that CHD4 acts in a gene- and signal-specific manner. Finally, we note that similar types of experiments targeted at BRG1, a functionally distinct SNF2-like ATPase found in BAF and PBAF chromatin remodeling complexes, interferes with different developmental processes (Seo et al. 2005; N. Singhal and R. Rupp, unpubl.). The phenotypes reported here are, therefore, specific consequences of the experimental alterations of CHD4 protein abundance.

The qualitatively indistinguishable phenotypes achieved either by Morpholino-mediated knockdown of endogenous CHD4 protein or overexpression of the dnCHD4 variant indicate a requirement for ATP hydrolysis and, thus, most likely involve alterations of the local chromatin structure at the *Sip1* locus. The molecular nature of these alterations is currently unknown, but probably depends on the protein context in which CHD4 becomes recruited to the *Sip1* gene. CHD4/Mi-2β has been purified biochemically as a component of the high-molecular-weight NuRD complex, which requires the help of other subunits to exert full nucleosome-remodeling activity (Becker and Hörz 2002). Recently, several NuRD complex variants have been purified that differ in their ability to interact with methylated DNA or other proteins (for details, see Bowen et al. 2004; Fujita et al. 2004; Brackertz et al. 2006; Le Guezennec et al. 2006). However, CHD4/Mi-2β has also been invoked in gene
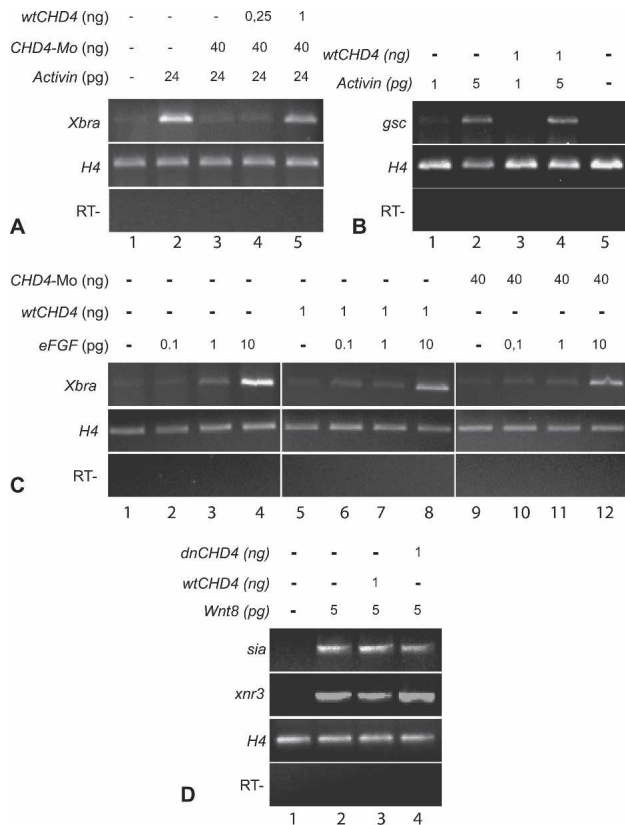
Figure 6. Specificity of CHD4-dependent threshold control. The specificity of the *Xbra* promoter response was further investigated in animal caps. (*A*) The *CHD4*-Mo-dependent desensitization of the *Xbra* promoter can be rescued by *wtCHD4* mRNA coinjection. (*B*) The Activin threshold of the *Gsc* promoter is not altered by *CHD4* overexpression. (*C*) Elevated or reduced CHD4 protein levels had no significant effect on the eFGF-dependent induction of *Xbra* transcription (cf. lanes *4*, *8*, and *12*). (*D*) Neither *wtCHD4* nor *dnCHD4* mRNA levels affect the induction of *Siamois* or *Xnodal related 3* by Wnt8/canonical Wnt signaling.

activation, either in a complex with the basic helix–loop–helix (bHLH) protein HEB and the histone acetyltransferase p300 on the CD4 gene during T-cell development (Williams et al. 2004), or in the form of protein supercomplexes containing both NuRD and SWI/SNF subunits (Shimono et al. 2003). Our ChIP results have established Sip1 as a direct CHD4 target (Fig. 4) and suggest an association of CHD4 protein with the actively transcribed *Sip1* gene body, because overexpression of CHD4 protein reduced *Sip1* mRNA levels in isolated animal caps (Fig. 2B). Based on this, we propose that a CHD4-containing protein complex—probably NuRD—suppresses *Sip1* expression by impeding transcription through nucleosome remodeling and/or HDAC-mediated hypoacetylation. It remains a formidable challenge for future investigations to identify the precise nature of the CHD4 protein complex and how it is recruited to the *Sip1* gene, as well as to investigate its mechanism of action at its preferred binding site around exon E1.

Related to our findings, the constitutive NuRD com-

ponent MBD3 has been shown to be required for pluripotency of murine embryonic stem cells (Kaji et al. 2006). Interestingly, MBD3$^{-/-}$ ES cells showed defects in gene silencing and were severely compromised in cell fate commitment. Our observations indicate that CHD4 loss of function prevented neither germ layer formation nor cell differentiation. However, MBD3 protein is essential for stable formation of the NuRD complex formation (Kaji et al. 2006), while Morpholino knockdown or overexpression of dnCHD4 will cause only a partial loss-of-function situation. While the apparent discrepancy between the two studies results probably from quantitative differences of NuRD inhibition, it suggests that there may be more functions to be discovered for this conserved chromatin remodeling machine.

Our results also add to the extraordinary complexity of the regulatory machinery underlying gene expression patterns such as the *Xbra* domain, whose superficially contiguous appearance is shaped by a plethora of positive and negative inputs (see also Heasman 2006; Kimelman 2006; Wardle and Smith 2006). Elegant experiments in *Xenopus* had provided insight into how the *Sip1* and *Xbra* domains become segregated during gastrulation, but had also indicated a requirement for additional mechanisms beyond the simple repression of the *Xbra* gene by Sip1 protein to explain this process (Lerchner et al. 2000; Papin et al. 2002). Our data add two important regulatory facets to this problem. First, the CHD4-dependent suppression of *Sip1* transcription is sufficient to tune the Activin/Nodal-response threshold of the *Xbra* promoter over a surprisingly broad concentration range in vitro (Fig. 5), and more importantly also under in vivo induction conditions (Figs. 1–3). Secondly, CHD4 does not significantly interfere with eFGF/MAPK-dependent stimulation of *Xbra* transcription. Together, this suggests that the CHD4/Sip1 epistasis is involved in restricting the primary, unstable induction of *Xbra*, but stops operating in presumptive mesodermal cells, in which Xbra has managed to engage the eFGF feedback loop. A major implication of these results is that chromatin remodeling factors such as CHD4/Mi-2β are part of the machinery that translates morphogen signals into spatial territories of gene expression patterns during vertebrate embryogenesis.

Materials and methods

Expression constructs and synthetic mRNAs

The ORF of *Xenopus* CHD4 was generated by PCR from an EST (BF047668; RZPD) and subcloned via BamHI/XhoI sites into the pCS2$^+$ vector (see Supplementary Fig. S3 for primer sequences). The dominant-negative CHD4 variant was constructed with a site mutagenesis kit (Stratagene) according to the manufacturer's instructions. In the same way, the *Xenopus* Sip1 ORF was subcloned into pCS2$^+$ using a cDNA clone as a template (Eisaki et al. 2000). Plasmids were linearized with Asp718 or NotI and transcribed with Sp6 RNA polymerase. Expression plasmids for eGFP, Activin, Wnt8, and eFGF have been described (Steinbach et al. 1997). For the production of rat monoclonal antibodies, the C-terminal domain of xCHD4 (amino acids 1513–1891) was

cloned into the pGEX-4T3 bacterial expression vector (Amersham), expressed in *Escherichia coli*, and purified as described (Linder et al. 1998).

Morpholino-mediated protein ablation

We used a 25-mer antisense Morpholino oligonucleotide complementary to the *Xenopus* CHD4 translation start (see Supplementary Fig. S2A). The unrelated, standard control Morpholino supplied by Gene Tools LLC served as a control for specificity (for sequences, see Supplementary Fig. S4). All Morpholinos were resuspended in distilled water and injected at a dose of 40 ng per embryo, unless stated otherwise. To test the efficiency of *CH4*-Mo, we subcloned the first 363 amino acids of CHD4 in-frame upstream of the 6xMyc-tag cassette of the pCS2 + MT6 vector, either with or without the 5′ untranslated region (UTR) complementary to the *CHD4*-Mo. In vitro translations of these test constructs (SP6-TNT-Kit; Pormega) were performed in the presence of increasing amounts of *CHD4*-Mo, followed by Western blot analysis using the 9E10 anti-Myc mAb to detect the relative levels of the CHD4-Myc protein. Sip1 mRNA translation was inhibited by the published Morpholino described by Nitta et al. (2004).

Embryo manipulations and analysis

Handling, culture, and staging of in vitro fertilized *Xenopus* embryos followed standard procedures (Sive et al. 2000). Microinjections of mRNA or Morpholinos were performed in 5 μL of volume into one blastomere of the two-cell stage for embryonic phenotypes, or with 4×2.5 μL into the animal pole of four-cell-stage embryos for preloading of animal cap tissue. CHD4 and Sip1 mRNAs were used at 1.0 ng/embryo, which had been defined as an optimal dose for functional interference without toxic side effects (data not shown). For further analysis, embryos were presorted into left-side- or right-side-injected specimens by coinjected eGFP lineage tracer before fixation.

Whole-mount RNA in situ hybridizations were performed as described (Sive et al. 2000) with Digoxigenin-labeled antisense RNA probes at concentrations ranging from 0.2 to 0.6 μg/mL. Color reactions with BM purple substrate (Roche) were stopped after 10–48 h at 16°C. Embryos were refixed in MEMFA, bleached, and photographed under bright light with a Progress C14 camera (Jenoptik) and a Leica MZIII stereoscope. Immunocytochemistry was performed with a *Xenopus* CHD4-specific monoclonal antibody and AP-conjugated sheep anti-rat secondary antibody. For histological sections, embryos were fixed in 4.5% formalin and embedded in paraffin. Six-micron sections were stained with hematoxylin and eosin and photographed using an Axiophot microscope (Zeiss).

Animal cap assay and RT–PCR

Animal caps were dissected with a gastromaster (yellow tip; Xenotek Engineering) at late blastula (7 h post-fertilization) and cultured in 0.5× MBS buffer on Agarose until mid-gastrula. RNA extraction and semiquantitative RT–PCR were performed as described (Steinbach and Rupp 1999). For real-time RT–PCR, we used the Power SYBR Green PCR Master Mix (Applied Biosystems) and the Abi 7000 Lightcycler (Applied Biosystems). The primer sequences are listed in Supplementary Figure S4.

ChIP

Embryo ChIP analysis (gastrula stage NF11) was performed as described by Chanas et al. (2004) with the following modifica-

tions: Two-hundred embryos were homogenized in 10 mL of buffer A1 containing 1% paraformaldehyde at 17°C in Douncer S (Braun). The chromatin was sheered to an average size of 300–1000 base pairs (bp) with the Bioruptor (Diagenode) and cleared by centrifugation for 5 min, 4000*g* at 4°C. The supernatant was transferred to a new tube. The pellet was re-eluted with 2 mL of buffer A2 containing 0.1% SDS and 0.5% Sarcosine, and supernatants were combined and cleared twice via centrifugation at 20,000*g* for 10 min. For immunoprecipitation with xCHD4-specific rat monoclonal antibodies, 30 μL of DNA/BSA-blocked Protein A-Sepharose bead slurry (Amersham Pharmacia) were precoupled for 60 min with 15 μg of rabbit anti-rat IgG antibodies (Dianova) and mouse anti-rat IgM antibodies (Biozol) in PBS at room temperature. The protein A-Sepharose was subsequently incubated with 10 mL of a mix of five different xCHD4-specifc monoclonal antibodies, and incubated for 4 h at room temperature. For preclearing, 50 μL of blocked protein A-Sepharose suspension were added to 1 mL of chromatin lysate and rotated for 1 h at 4°C. Lysate aliquots of 100 embryo equivalents were incubated rotating overnight at 4°C with 3 μL of Protein A-Sepharose, which was either preabsorbed with xCHD4-specific antibody mix or with bridging antibodies as a control for unspecific binding. The protein A-Sepharose samples with bound chromatin fragments were pelleted by centrifugation for 1 min at 2000 rpm and washed sequentially by 15 min of rotation at 4°C with 1 mL of buffer A2 containing 0.1% SDS (four washes), 500 mM NaCl and 0.1% SDS (one wash), and TE (two washes). The chromatin was eluted and the DNA was purified as described (Fujita et al. 2004). The final DNA pellets were dissolved in 50 μL of ddH_2O, and 2-μL aliquots were added to each PCR reaction, carried out as duplicates. The *Xenopus* Sip1 Taqman amplicons (for primers and probes, see Supplementary Fig. S4) were based on published cDNA sequence (Eisaki et al. 2000). Exons U5, E1, and E2 were identified by sequence conservation between *Xenopus tropicalis* (genome assembly version 4.1, scaffold 232) and mouse (Nelles et al. 2003) *sip1* genomic DNA sequences. The relative occupancy of CHD4 protein at the *sip1* locus was calculated by sequential normalization to the input and to the GAPDH control amplicon.

References

Becker, P.B. and Hörz, W. 2002. ATP-dependent nucleosome remodeling. *Annu. Rev. Biochem.* **71:** 247–273.

Bowen, N.J., Fujita, N., Kajita, M., and Wade, P.A. 2004. Mi-2/NuRD: Multiple complexes for many purposes. *Biochim. Biophys. Acta* **1677:** 52–57.

Brackertz, M., Gong, Z., Leers, J., and Renkawitz, R. 2006. p66α and p66β of the Mi-2/NuRD complex mediate MBD2 and histone interaction. *Nucleic Acids Res.* **34:** 397–406.

Casey, E.S., O'Reilly, M.A., Conlon, F.L., and Smith, J.C. 1998. The T-box transcription factor Brachyury regulates expres-

sion of eFGF through binding to a non-palindromic response element. *Development* **125:** 3887–3894.

Chanas, G., Lavrov, S., Iral, F., Cavalli, G., and Maschat, F. 2004. Engrailed and polyhomeotic maintain posterior cell identity through cubitus-interruptus regulation. *Dev. Biol.* **272:** 522–535.

Cunliffe, V. and Smith, J.C. 1992. Ectopic mesoderm formation in *Xenopus* embryos caused by widespread expression of a *Brachyury* homologue. *Nature* **358:** 427–430.

De Robertis, E.M. and Kuroda, H. 2004. Dorsal–ventral patterning and neural induction in *Xenopus* embryos. *Annu. Rev. Cell Dev. Biol.* **20:** 285–308.

Eisaki, A., Kuroda, H., Fukui, A., and Asashima, M. 2000. XSip1, a member of the two-handed zinc finger proteins, induced anterior neural markers in *Xenopus laevis* animal cap. *Biochem. Biophys. Res. Commun.* **271:** 151–157.

Fujita, N., Jaye, D.L., Kajita, M., Geigermann, C., Moreno, C.S., and Wade, P.A. 2003. MTA-3, a Mi-2/NuRD complex subunit, regulates an invasive growth pathway in breast cancer. *Cell* **113:** 207–219.

Fujita, N., Jaye, D.L., Geigermann, C., Akyldiz, A., Mooney, M.R., Boss, J.M., and Wade, P.A. 2004. MTA-3 and the Mi-2/NuRD complex regulate cell fate during B lymphocyte differentiation. *Cell* **119:** 75–86.

Furlow, J.D. and Brown, D.D. 1999. In vitro and in vivo analysis of the regulation of a transcription factor gene by thyroid hormone during *Xenopus laevis* metamorphosis. *Mol. Endocrinol.* **13:** 2076–2089.

Green, J. 1999. The animal cap assay. In *Molecular methods in developmental biology*—Xenopus *and* zebrafish (ed. M. Guille), Vol. 127, pp. 1–14. Humana Press, Totowa, NJ.

Green, J. 2002. Morphogen gradients, positional information, and *Xenopus*: Interplay of theory and experiment. *Dev. Dyn.* **225:** 392–408.

Heasman, J. 2006. Patterning the early *Xenopus* embryo. *Development* **133:** 1205–1217.

Heasman, J., Kofron, M., and Wylie, C. 2000. β-Catenin signalling activity dissected in the early *Xenopus* embryo: A novel antisense approach. *Dev. Biol.* **222:** 124–134.

Kaji, K., Caballero, I.M., MacLeod, R., Nichols, J., Wilson, V.A., and Hendrich, B. 2006. The NuRD component Mbd3 is required for pluripotency of embryonic stem cells. *Nat. Cell Biol.* **8:** 285–292.

Kehle, J., Beuchle, D., Treuheit, S., Christen, B., Kennison, J.A., Bienz, M., and Muller, J. 1998. dMI-2, a hunchback-interacting protein that functions in polycomb repression. *Science* **282:** 1897–1900.

Kimelman, D. 2006. Meoderm induction: From caps to chips. *Nat. Rev. Genet.* **7:** 360–372.

Kurth, T., Meissner, S., Schäckel, S., and Steinbeisser, H. 2005. Establishment of Mesodermal gene expression patterns in early *Xenopus* embryos: The role of repression. *Dev. Dyn.* **233:** 418–429.

Kwan, K.M. and Kirschner, M.W. 2003. Xbra functions as a switch between cell migration and convergent extension in the *Xenopus* gastrula. *Development* **130:** 1961–1972.

Latinkic, B.V., Umbhauer, M., Neal, K.A., Lerchner, W., Smith, J.C., and Cunliffe, V. 1997. The *Xenopus* Brachyury promoter is activated by FGF and low concentrations of activin and suppressed by high concentrations of activin and by paired-type homeodomain proteins. *Genes & Dev.* **11:** 3265–3276.

Le Guezennec, X., Vermeulen, M., Brinkman, A.B., Hoeijmakers, W.A., Cohen, A., Lasonder, E., and Stunnenberg, H.G. 2006. MBD2/NuRD and MBD3/NuRD, two distinct complexes with different biochemical and functional properties.

Mol. Cell. Biol.* **26:** 843–851.

Lerchner, W., Latinkic, B.V., Remacle, J.E., Huylebroeck, D., and Smith, J.C. 2000. Region-specific activation of the *Xenopus* Brachyury promotor involves active repression in ectodermand endoderm: A study using transgenic frogs. *Development* **127:** 2729–2739.

Linder, B., Jones, L.K., Chaplin, T., Mohdsarip, A., Heinlein, U.A.O., Young, B.D., and Saha, V. 1998. Expression pattern and cellular distribution of the murine homologue of AF10. *Biochim. Biophys. Acta* **1443:** 285–296.

Linder, B., Cabot, R.A., Schwickert, T., and Rupp, R.A. 2004. The SNF2 domain protein family in higher vertebrates displays dynamic expression patterns in *Xenopus laevis* embryos. *Gene* **326:** 59–66.

Loose, M. and Patient, R. 2004. A genetic regulatory network for *Xenopus* mesendoderm formation. *Dev. Biol.* **271:** 467–478.

Nelles, L., Van de Putte, T., van Grunsven, L., Huylebroeck, D., and Verschueren, K. 2003. Organization of the mouse Zfhx1b gene encoding the two-handed zinc finger repressor Smad-interacting protein-1. *Genomics* **82:** 460–469.

Niehrs, C. 2004. Regionally specific induction by the Spemann-Mangold organizer. *Nat. Rev. Genet.* **5:** 425–434.

Nitta, K.R., Tanegashima, K., Takahashi, S., and Asashima, M. 2004. XSIP1 is essential for early neural gene expression and neural differentiation by suppression of BMP signaling. *Dev. Biol.* **275:** 258–267.

Papin, C., van Grunsven, L.A., Verschueren, K., Huylebroeck, D., and Smith, J.C. 2002. Dynamic regulation of Brachyury expression in the amphibian embryo by XSIP1. *Mech. Dev.* **111:** 37–46.

Postigo, A.A. and Dean, D.C. 1997. ZEB, a vertebrate homolog of *Drosophila* Zfh-1, is a negative regulator of muscle differentiation. *EMBO J.* **16:** 3935–3943.

Richmond, E. and Peterson, C.L. 1996. Functional analysis of the DNA-stimulated ATPase domain of yeast SWI2/SNF2. *Nucleic Acids Res.* **24:** 3685–3692.

Schohl, A. and Fagotto, F. 2002. β-Catenin, MAPK and Smad signaling during early *Xenopus* development. *Development* **129:** 37–52.

Seo, S., Richardson, G.A., and Kroll, K.L. 2005. The SWI/SNF chromatin remodeling protein Brg1 is required for vertebrate neurogenesis and mediates transactivation of Ngn and NeuroD. *Development* **132:** 105–115.

Sheng, G., dos Reis, M., and Stern, C.D. 2003. Churchill, a Zn finger transcriptional activator, regulates the transition between gastrulation and neurulation. *Cell* **115:** 603–613.

Shimono, Y., Murakami, H., Kawai, K., Wade, P.A., Shimokata, K., and Takahashi, M. 2003. Mi-2 β associates with BRG1 and RET finger protein at the distinct regions with transcriptional activating and repressing abilities. *J. Biol. Chem.* **278:** 51638–51645.

Sive, H.L., Grainger, R.M., and Harland, R.M. 2000. *Early development of* Xenopus laevis*. A laboratory manual.* Cold Spring Harbor Laboratory Press, Cold Spring Harbor, NY.

Stancheva, I., Collins, A.L., Van den Veyver, I.B., Zoghbi, H., and Meehan, R.R. 2003. A mutant form of MeCP2 protein associated with human Rett syndrome cannot be displaced from methylated DNA by notch in *Xenopus* embryos. *Mol. Cell* **12:** 425–435.

Steinbach, O.C. and Rupp, R.A.W. 1999. mRNA quantitation by reverse transcription/polymerase chain reaction (RT/PCR). In *Molecular methods in developmental biology*—Xenopus *and zebrafish* (ed. M. Guille), Vol. 127, pp. 41–56. Humana Press, Totowa, NJ.

Steinbach, O.C., Wolffe, A.P., and Rupp, R.A.W. 1997. Somatic linker histones cause loss of mesodermal competence in

Xenopus. Nature **389:** 395–399.

Stern, C.D. 2005. Neural induction: Old problem, new findings, yet more questions. *Development* **132:** 2007–2021.

Unhavaithaya, Y., Shin, T.H., Miliaras, N., Lee, J., Oyama, T., and Mello, C.C. 2002. MEP-1 and a homolog of the NURD complex component Mi-2 act together to maintain germline–soma distinctions in *C. elegans*. *Cell* **111:** 991–1002.

Verschueren, K., Remacle, J.E., Collart, C., Kraft, H., Baker, B.S., Tylzanowski, P., Nelles, L., Wuytens, G., Su, M.T., Bodmer, R., et al. 1999. SIP1, a novel zinc finger/homeodomain repressor, interacts with Smad proteins and binds to 5′-CACCT sequences in candidate target genes. *J. Biol. Chem.* **274:** 20489–20498.

von Zelewsky, T., Palladino, F., Brunschwig, K., Tobler, H., Hajnal, A., and Muller, F. 2000. The *C. elegans* Mi-2 chromatin-remodelling proteins function in vulval cell fate determination. *Development* **127:** 5277–5284.

Wade, P.A., Gegonne, A., Jones, P.L., Ballestar, E., Aubry, F., and Wolffe, A.P. 1999. Mi-2 complex couples DNA methylation to chromatin remodeling and histone deacetylation. *Nat. Genet.* **23:** 62–66.

Wakamatsu, N., Yamada, Y., Yamada, K., Ono, T., Nomura, N., Tanigochi, H., Kitoh, H., Mutoh, N., Yamanaka, T., Mushiake, K., et al. 2001. Mutations in SIP1, encoding Smad interacting protein-1, cause a form of Hirschsprung disease. *Nat. Genet.* **27:** 369–370.

Wardle, F.C. and Smith, J.C. 2006. Transcriptional regulation of mesendoderm formation in *Xenopus. Semin. Cell Dev. Biol.* **17:** 99–109.

Williams, C.J., Naito, T., Arco, P.G., Seavitt, J.R., Cashman, S.M., De Souza, B., Qi, X., Keables, P., Von Andrian, U.H., and Georgopoulos, K. 2004. The chromatin remodeler Mi-2β is required for CD4 expression and T cell development. *Immunity* **20:** 719–733.